EUROPEAN ORGANIZATION FOR NUCLEAR RESEARCH

# SOME PROPERTIES OF SPHERICAL DRIFT CHAMBERS

G. Charpak, C. Demierre, R. Kahn, J.C. Santiard and F. Sauli

CERN, Geneva, Switzerland

## ABSTRACT

A large-aperture X-ray imaging chamber is described. Angular aperture: 90°. Thickness of spherical absorbing drift space: 10 cm. The photoelectron's position is measured in a proportional chamber of 50 × 50 $cm^2$, with an accuracy of 0.8 mm (FWHM) in all coordinates.

Geneva - 12 November 1976

(Submitted to Nuclear Instruments and Methods)

# SOME PROPERTIES OF SPHERICAL DRIFT CHAMBERS

G. Charpak, C. Demierre, R. Kahn, J.C. Santiard and F. Sauli

CERN, Geneva, Switzerland

## 1. INTRODUCTION

We have investigated the properties of a spherical drift chamber[1] aimed at measuring the angular distribution of soft X-rays emitted by a point source, crystal or pinhole.

The characteristics of the chamber are the following (Fig. 1):

a) Drift space D

- Entrance electrode: spherical shape, aluminium of 40 μm thickness, radius 18 cm.
- Exit electrode: spherical shape, stainless steel grid of 82% transparency, radius of 28 cm.
- Angular acceptance: 90°.

b) Transfer space T

- Minimum thickness, on the central axis: 2.5 cm; maximum thickness, at 45°: 10 cm.

c) Read-out proportional chamber C

- Dimensions: 50 cm × 50 cm.
- Anode wire spacing: 1 mm or 2 mm, of 10 μm diameter gold-plated tungsten; or 2 mm, of 20 μm diameter gold-plated tungsten.
- Cathode wires spacing: 1 mm, of 50 μm diameter bronze beryllium.
- Anode-cathode distance: 6 mm.
- Read-out method: analog computation of avalanche centroid.

## 2. THE PROPORTIONAL CHAMBER

The chamber is made of a plane of anode wires sandwiched between cathode planes and at a distance of 6 mm from each. The cathode planes are made of wires of 50 μm diameter, spaced by 1 mm, parallel to the anode wires in the entrance face and orthogonal to it in the back plane. The wires are connected together by groups of 6. The pulses induced in every strip are mixed together in

parallel in an analogic circuit measuring the centre of gravity of the induced pulse; this device is an extension to 72 channels of a previous one with 36 channels[2]. The total time required for the two-dimensional read-out of the coordinates of an avalanche is 5 μsec.

The accuracy is somehow better than 1 mm, which was initially aimed at for this chamber. It first appeared that the limit for the accuracy would be set by the anode wire spacing which was planned to be of 1 mm.

Many inconveniencies were connected with such a wire spacing. To overcome the electrostatic instabilities we had to have nylon strings supporting the anode wires every 10 cm. This introduced dead regions which are a nuisance in an instrument of this kind. The operation was also very delicate and wire breaking was a common failure. We finally discovered that because of the diffusion in the drift space, the electron clouds always shared their charge between two wires, even at 2 mm wire spacing, thus permitting an interpolation between wires. We then gave up the 1 mm wire spacing and with 2 mm wire spacing the accuracy is still well below 1 mm, as we will see. This paved the way for chambers of a much simpler construction, with anode wires of 20 μm diameter, spaced at 2 mm. As is well known from high-energy physics practice, chambers of several square metres can be easily built with such parameters; they still give a localization accuracy much better than the wire spacing, if they are connected to a drift space of sufficient thickness to spread the initial electron cloud to dimensions larger than a wire spacing.

While the experiments are far from being completed, many other interesting properties, to some extent surprising, have appeared in the preliminary study which we present here. Whilst the chamber is intended to be used with a mixture rich in xenon, these studies were conducted with a flowing mixture commonly used in multiwire chambers: argon (70%), isobutane (28%), methylal (2%). The use of argon, instead of xenon, is advantageous at this stage since only a fraction of the X-rays is absorbed in the drift space, typically 60% at 8 keV; we can thus compare the transport properties of the different spaces by controlling separately the voltages applied to them. When we studied the variation of the pulse height as a function of the fields in D and T, it appeared that the results were dependent on the voltage of the chamber. The striking phenomenon was that beyond a given voltage in the chamber the pulses generated by photoelectrons which had transited through the drift space were larger and of better resolution than those from photoelectrons produced in the chamber.

This is clearly illustrated by the curves of Fig. 2. The variation of the average pulse height as a function of voltage is shown in Fig. 3. The curve obtained without drifting is approximate since the resolution becomes very poor as

the voltage in the chamber increases and the peak is badly defined. We thus see that one advantage of having the photoelectron drifting before reaching the anode wire is that higher amplification can be reached in the linear region than in a thin proportional counter.

## 3. THE TRANSFER SPACE

The transfer space is the weakest part of the system since the electrical field varies by a factor of 4 from centre to edge.

By applying a reverse field on the drift space one can study the pulses from X-rays absorbed only in T. Figure 4 shows the pulse height from 8 keV X-rays, as a function of applied voltage, for different directions of a beam of X-rays; at 0° incidence (on the central axis) we see that the pulse height is decreasing by about 10% from 5 kV to 15 kV. This is a consequence of a change in the electrical transparency for electrons crossing the cathode plane, due to the different ratio of the fields on the two sides.

At 40° inclination of the X-ray beam, the pulse height increases smoothly but steadily and does not saturate at the maximum possible voltage on T, limited by discharges to about 20 kV. The interpretation is not clear. With increasing voltage both the path length and the size of the electron cloud change; because of the electron diffusion the cloud size is slightly reduced as the field increases. This does not, however, explain the increase in pulse height. The change in energy resolution is also interesting; it degrades slightly from 13% to 18% for the central part, thus confirming a loss of electrons as the field in the transfer space increases, and it improves from 42% to 18% at 40°, indicating a higher efficiency of electron collection. From 10 kV to 15 kV we have a region where the resolution is ranging from 15% to 18% for 8 keV X-rays at a given angle, with a pulse-height spread not exceeding 20% from 0 to 40°.

At 3.7 kV we have repeated this study. At 0°, the diffusion in T is insufficient to spread the electron cloud enough to escape space-charge saturation and the energy resolution is so bad that the measurements are too imprecise. At 40°, the resolution is good because of the diffusion introduced by the larger path length.

The pulse height varies exactly as at 3.3 kV, although the absolute value is about 5 times larger, thus confirming that thanks to the long drift space the space-charge effects occurring at 3.7 kV for photoelectrons which have diffused is unimportant. The energy resolution of about 18% to 20% is roughly the same between 10 and 15 kV and somehow better at smaller voltages than with a voltage of 3.3 kV in the chamber.

## 4. THE DRIFT SPACE

We have not studied the variation of the collection efficiency as a function of the field in D, with a constant field in T, but varied the two simultaneously, with a chain of resistances giving the sharing in the total potential between D and T. The sharing has been varied. The response of the chamber to a beam of 8 keV X-rays, collimated to about 1 mm and centred in the chamber, varies with angle and with applied voltage, in a way which we think can be interpreted. Some typical spectra for a total voltage of 26 kV, where 11 kV are applied to the drift space and 15 kV to the transfer space, are seen on Fig. 5, with 3.7 kV on chamber C.

As a function of total voltage, the pulse height and resolution vary (Fig. 6). At a total voltage of 26 kV, the resolution is acceptable at 0° (17%). The peak is symmetric, with no ghost peaks. At 20° the pulse height reaches the same value as at 0°, with a slightly worse resolution, 19% at 26 kV. But as we increase the angle a second peak appears clearly. At 40° we are on a rather steep slope for the pulse height, even at 26 kV total voltage, and we reach only 70% of the value found at 0° and 20°. Since at 15 kV on the transfer voltage (which corresponds to 26 kV total voltage) we reach the same pulse height at 0° and 40°, we may conclude that this loss of 30% occurs when the electrons cross the spherical grid between D and T. The occurrence of the second peak is a function of angle. It is suppressed, at 0°, by the space-charge effect, since it comes from those photons which have been absorbed in the shortest thickness of T or in C.

At 40°, the path length for the photoelectrons absorbed in T is longer and the amplification is higher (Figs. 2 and 3). These effects are not important if the X-rays are totally absorbed in D.

## 5. SPATIAL RESOLUTION

The spatial resolution was studied in the chamber before it was in its final form. The wires were 10 μm thick instead of 20 μm as in the final version and the wire spacing was the same, namely 2 mm. It had nylon strings every 10 cm. It was just the 1 mm spacing chamber with 1 wire out of two removed. When the $^{55}Fe$ source emitting the 5.9 keV photons is placed against the chamber, the localization in the direction orthogonal to the wires shows the pattern of wires distant by 2 mm with a FWHM of about 0.7 mm (Fig. 7a). If the source is placed at the focus of the drift chamber, the pattern disappears and the response is continuous (Fig. 7b). The question is whether the resolution has been spoiled or whether we are now interpolating between wires; to answer this question we have used a collimator of 0.1 mm diameter on our X-ray generator, which we could direct at all angles through the focal point of the spherical chamber.

Figure 8 shows the centroid positions in the directions perpendicular to the wires (a and b) and parallel to them (c), and in the direction parallel to the wires when the beam is not centred (d). The striking feature is that the accuracy is the same in all directions, within our accuracy measurement of 0.7 mm (FWHM). In other words, the electron cloud, which is initially of an extension well below 100 μm when it is produced, increases by diffusion and reaches a size larger than the wire spacing. This ensures the energy sharing between wires and permits an accuracy much better than the wire spacing.

An image was made with the chamber working as a pinhole camera with a hole of 1 mm diameter in a thin gold foil at the focus. The X-ray source was $^{55}Fe$ deposited in the grooves of a plastic foil featuring the word "CERN". The image (Fig. 9) displayed by the computer was exactly the one obtained by autoradiography except that it was enlarged by a factor of 6. The nylon string supporting the wire is visible.

The chamber was tested with a crystal of $CuV_2S_4$ of 0.5 mm width (spatial group Fd3m, a = 9.801 Å), rotating at the centre. Figure 10 shows the computer display of the two-dimensional coordinates of photons at a fixed crystal position. The reflections $00\bar{4}$ and $\bar{3}11$ are clearly visible. Figure 11a shows a slice of the distribution in the vertical direction (parallel to the wires) across the reflection $00\bar{4}$, and Fig. 11b that in the nearly horizontal direction (orthogonal to the wires) of the $\bar{3}11$ reflection.

We see that the resolution is around 1 mm (FWHM). The angles of reflection being rather large (36.7° and 30.2°), we see that the quality of large-aperture chambers is encouraging.

## 6. FURTHER DEVELOPMENTS: THE "ZOOM" X-RAY CAMERA

Our results show that a considerable accuracy, much better than the wire spacing, can be achieved if the electrons are given sufficient path length in the drift space to bring the electron cloud produced by a photoelectron to a size of the order of the wire spacing. This renders very easy the construction of large surface chambers. Our method of local measurement of the charge centroid keeps the accuracy to a level almost independent of chamber size. The electronic method which we use for the computation may have to be abandoned in favour of more accurate fast digital calculations[3]. The critical part is the difficulty to make spherical electrodes with large radii and large surfaces.

We have investigated two ways of overcoming this difficulty:

i) The rise-time of the pulse detected in a drift chamber with parallel electrodes is a function of the distance travelled by the electron cluster. We have found[4] that, with 5.9 keV photoelectrons produced in our gas mixture,

an accuracy of around 40% FWHM of the drift length can be achieved, up to 8 cm total drift. This is far from being good enough to compete with spherical drift chambers.

ii) In a flat electrode structure, electrical fields of any orientation can be obtained if the limiting electrodes are made of insulators covered with thin conducting lines at proper potentials.

The same lines of force as in cylindrical or spherical structures can then be obtained with flat electrodes. These are of much simpler construction, they are appropriate to large surfaces, and they have the considerable advantage of adjustable focal length. Such structures are under investigation.

## 7. CONCLUSIONS

In drift spaces of large dimensions, the diffusion of electrons spreads the initial cloud of ionization electrons. This presents two advantages:

- The primary electrons can give independent avalanches on the anode wires, and much larger gains can be obtained without space-charge saturation.
- The electron cloud can share its charge among two wires, at least, thus permitting the interpolation of the position between the wires. This facilitates considerably the construction of large-size chambers of high accuracy.
- One disadvantage of the spreading of the electrons may be a reduction of the maximum permissible counting rate, since a larger length of the wire is concerned by every pulse. However, as long as one stays in a linear region it is not clear how it compares with the case of strong local space-charge saturation effects, where the wire is dead over small distances of about 0.2 mm for tens of microseconds.

## Acknowledgements

We are indebted to Dr. A. Breskin for his help in the measurements of the chamber properties, and to R. Bouclier for many contributions to the development of the chamber. The spherical chambers were designed and built by R. Benoît and N. Greguric, who had to overcome many delicate mechanical problems, which will be described in a separate paper.

REFERENCES

1) G. Charpak, Z. Hajduk, A. Jeavons, R. Stubbs and R. Kahn, Nuclear Instrum. Methods 122, 307 (1974).

2) C. Demierre and G. Vuilleumier, Proc. 2nd Ispra Symposium on Nuclear Electronics, Stresa, 1975 (EUR 5370e, EURATOM, Luxemburg, 1975), p. 151.

3) A. Jeavons, N. Ford, B. Lindberg, C. Parkman and Z. Hajduk, IEEE Nuclear Sci. NS23, No. 1, 259 (1976).

4) A. Breskin, G. Charpak and F. Sauli, Nuclear Instrum. Methods 136, 497 (1976).

Figure captions

Fig. 1 : Spherical drift chamber. Angular aperture: 90°. Drift length: 10 cm. Radii of the entrance and exit electrodes: 18 cm and 28 cm, respectively. MWPC: wire spacings of 1 mm and 2 mm, 50 × 50 $cm^2$.

Fig. 2 : Space-charge effects. Pulse-height distributions from X-rays of 5.9 keV absorbed directly in the chamber (top curves) or after drifting through a spherical chamber (bottom curves) at two voltages: 3.3 kV and 3.7 kV.

Fig. 3 : Space-charge effects. Pulse height variation as a function of voltage on the chamber C for 8 keV photons absorbed in C or in D. 18 kV total voltage.

Fig. 4 : Absorption and transmission by transfer region T. 3.3 kV on C. 8 keV X-rays at two angles, 0° and 40°.

Fig. 5 : Response of spherical chamber to 8 keV photons. HV on C: 3.7 kV. Total voltage: 26 kV (15 kV on T). At 40°, the second peak is due to X-rays absorbed in T. At 0° their pulse height is reduced by space-charge saturation.

Fig. 6 : Response of spherical chamber to 8 keV photons. Pulse height and resolution variation as a function of the total applied voltage.

Fig. 7 : Localization in the spherical chamber. Source of $^{55}Fe$; a) against C, b) at the focus S of the spherical chamber.

Fig. 8 : Accuracy of the spherical chamber. Beam of 8 keV, collimator 0.1 mm. 11 channels = 2 mm. 20 kV total drift.
a) 0°. Coordinates orthogonal to anode wires.
b) Edge of chamber ∿ 42.5°. Coordinates orthogonal to anode wires.
c) Edge of chamber ∿ 42.5°. Coordinates parallel to wires, beam through centre.
d) Edge of chamber ∿ 42.5°. Coordinates parallel to wires, beam out of centre.
FWHM ∿ 0.7 mm in all directions. 0.5 mm accounted for by centroid read-out electronics.

Fig. 9 : Image of an X-ray source. A solution of $^{55}Fe$ is deposited on letters grooved in a plastic foil. Vertical letter size: 8 mm. Source at 5 cm from a pinhole of 1 mm diameter in a gold foil. Magnification factor: 6.

Fig. 10 : Diffraction pattern in a $CuV_2S_4$ crystal. Drift voltage: 12 kV. Transfer voltage: 12 kV. HV on the chamber 3.8 kV. Cross at centre. Pattern at a fixed angular position. Bottom reflection $00\bar{4}$, top left reflection $\bar{3}11$.

Fig. 11 : Diffraction spot width in a $CuV_2S_4$ crystal. Drift voltage: 12 kV. Transfer voltage: 12 kV. HV on chamber: 3.8 kV. Reflection $00\bar{4}$: $2\theta_B = 36.7°$ ($\theta_B$ = Bragg angle).

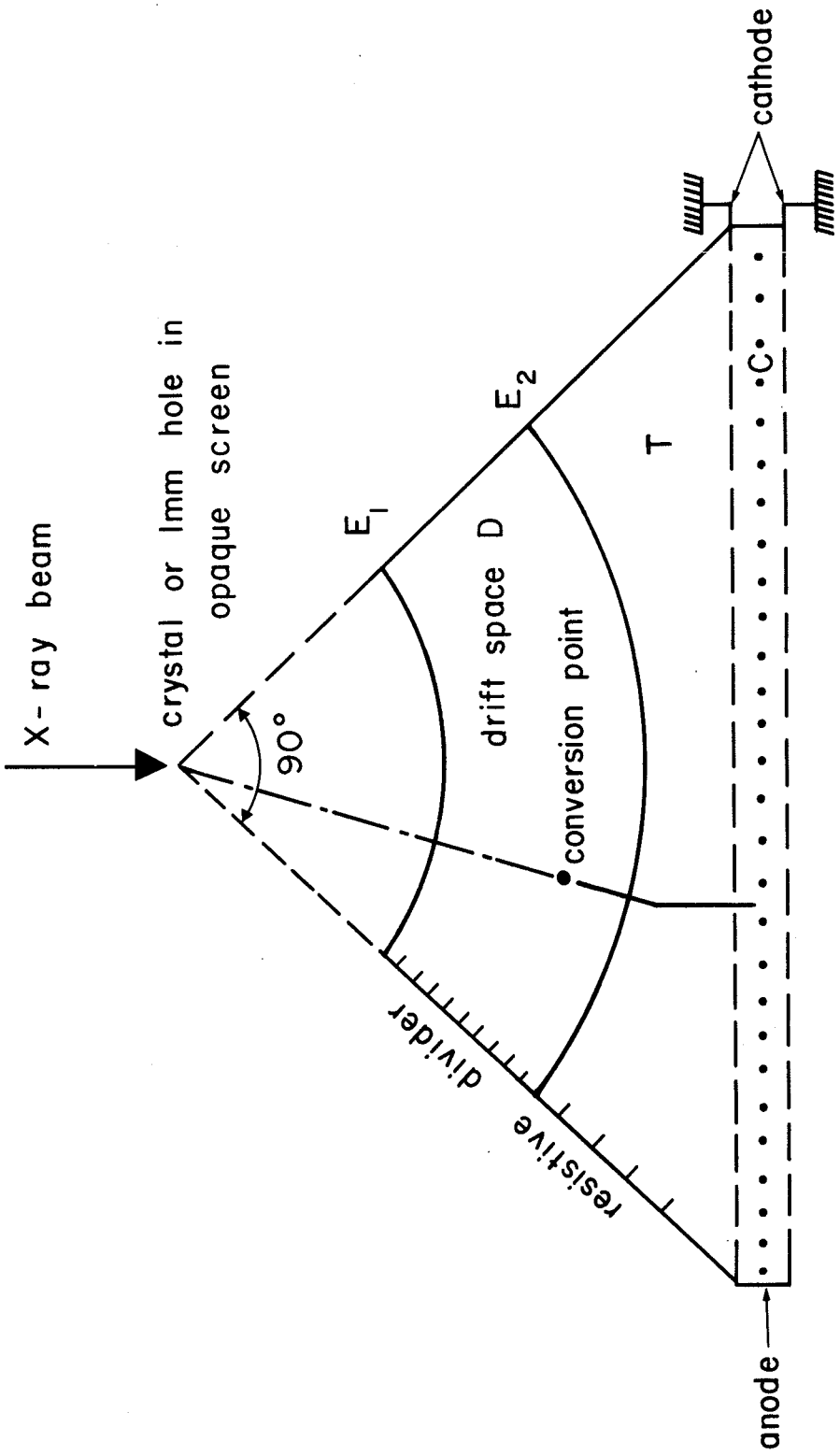


Fig. 1

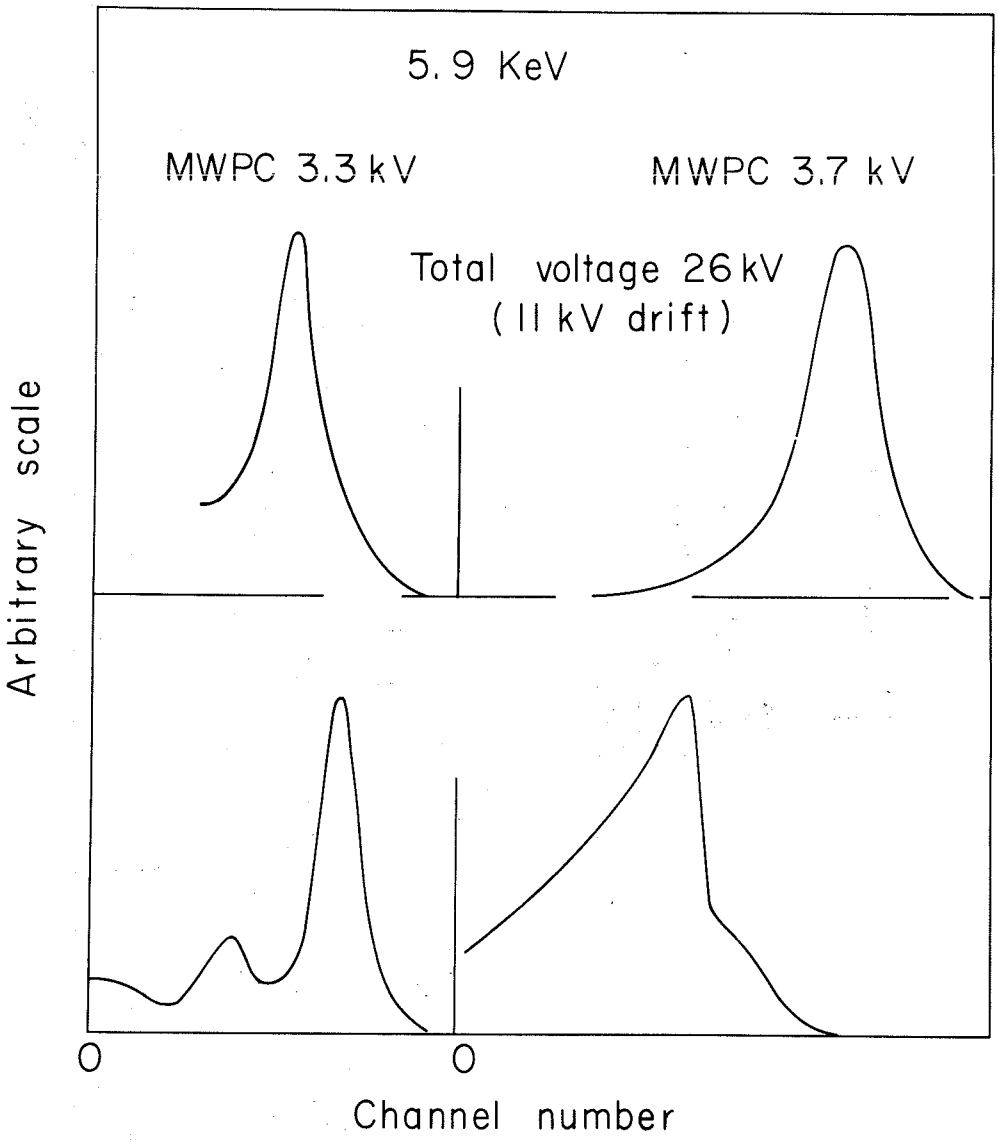


Fig. 2

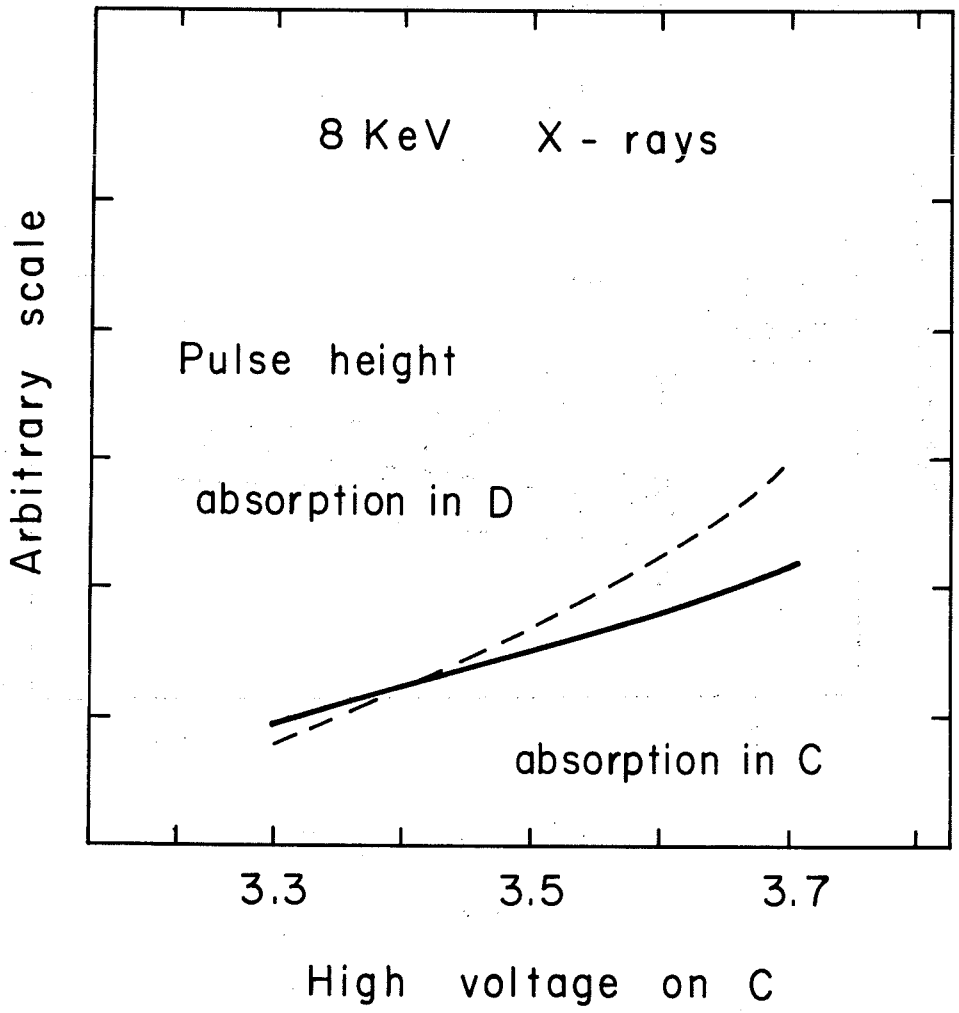


Fig. 3

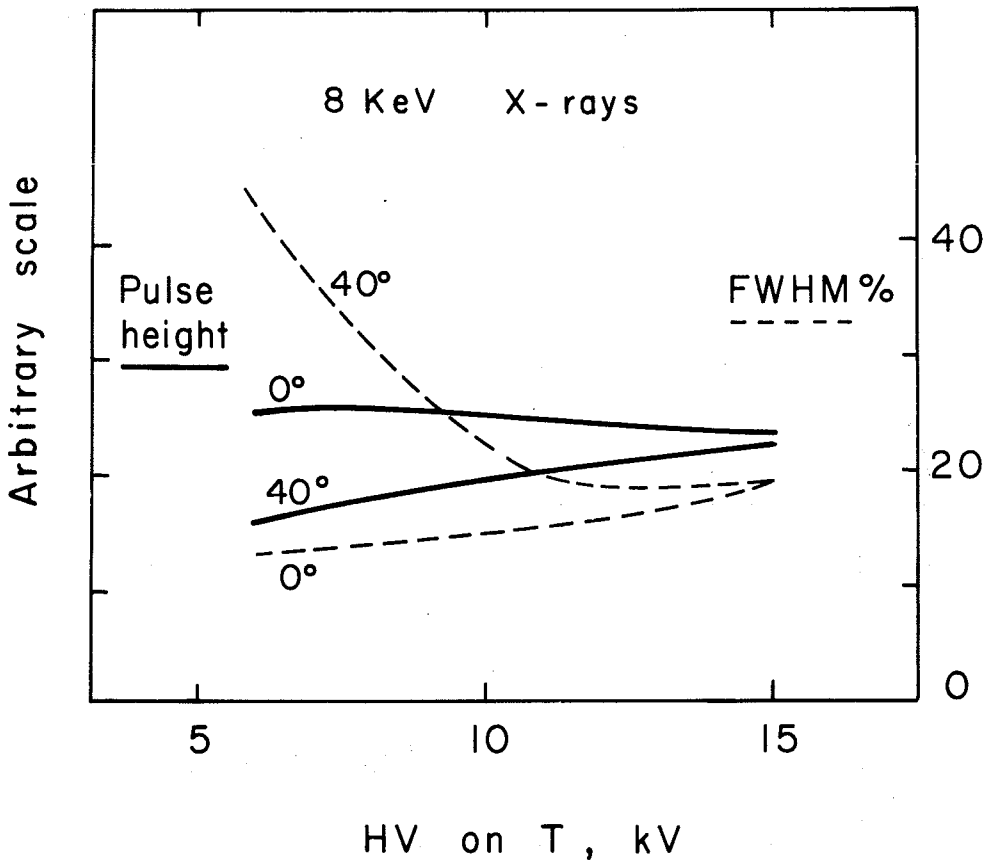


Fig. 4

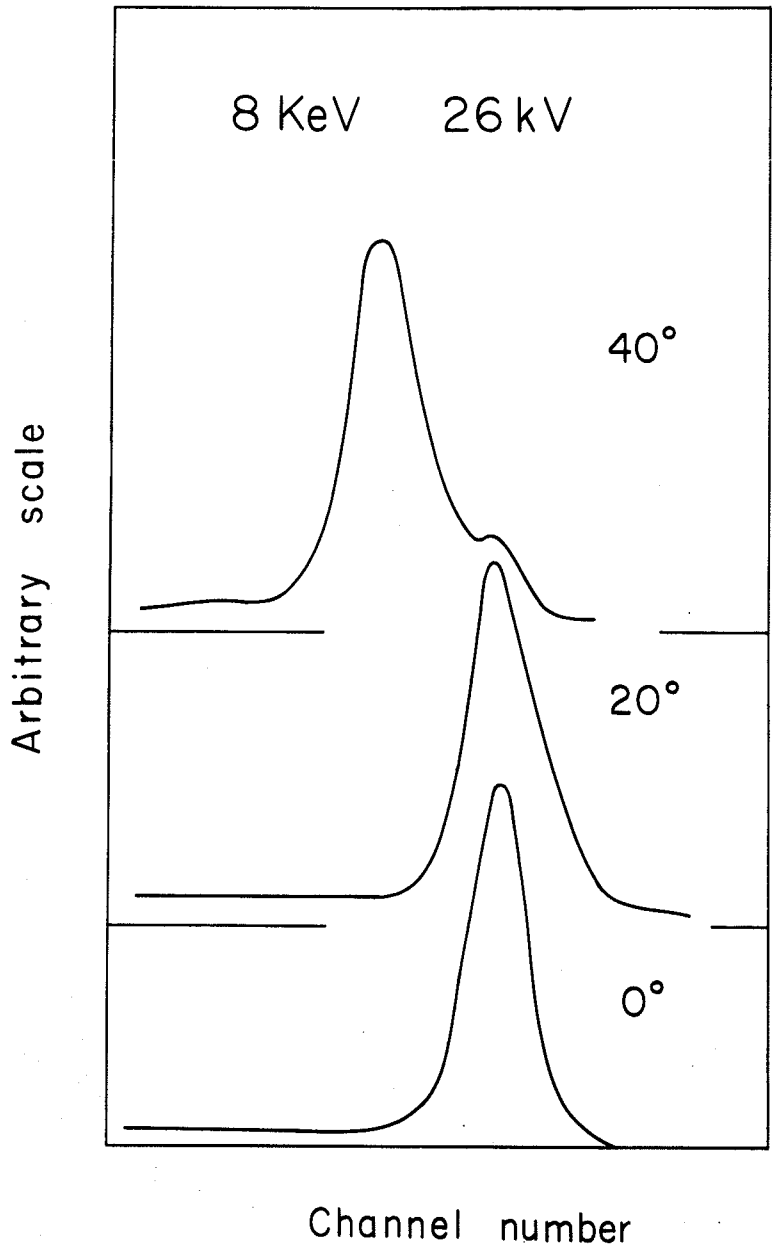


Fig. 5

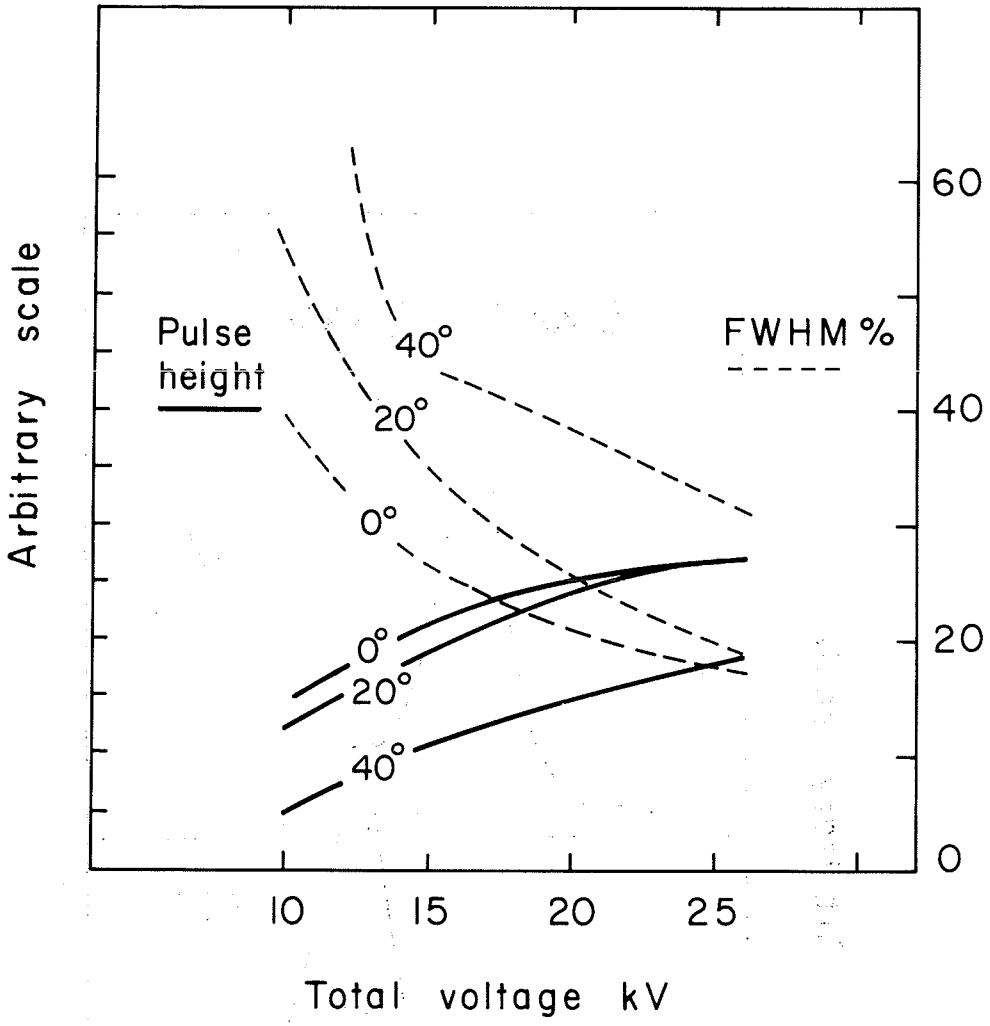


Fig. 6

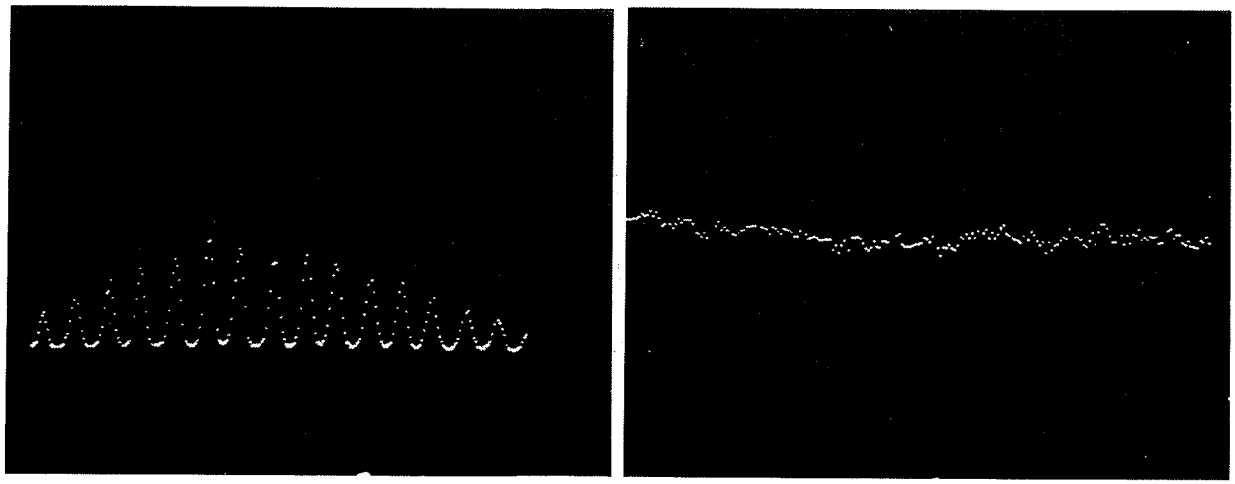

a) b)

Fig. 7

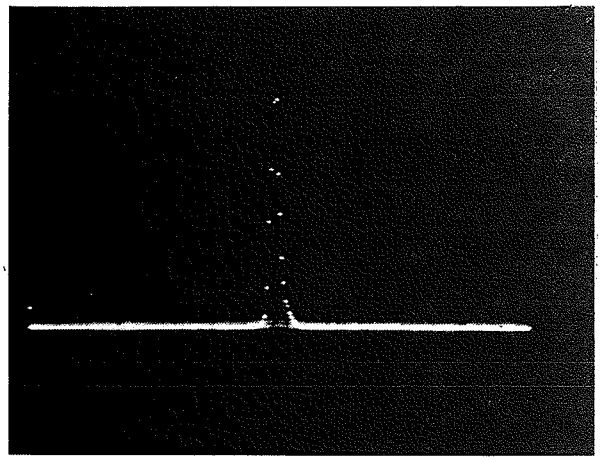

a)

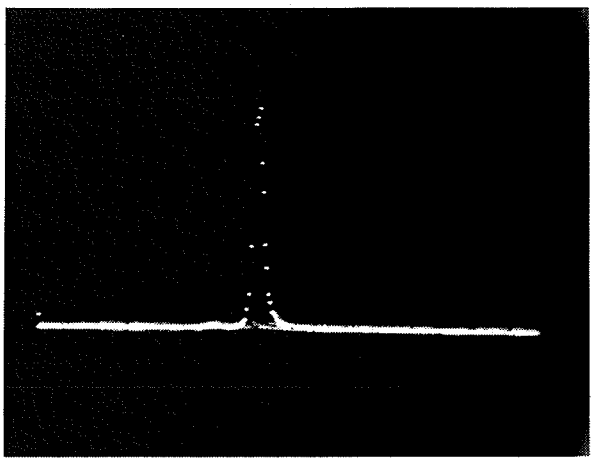

b)

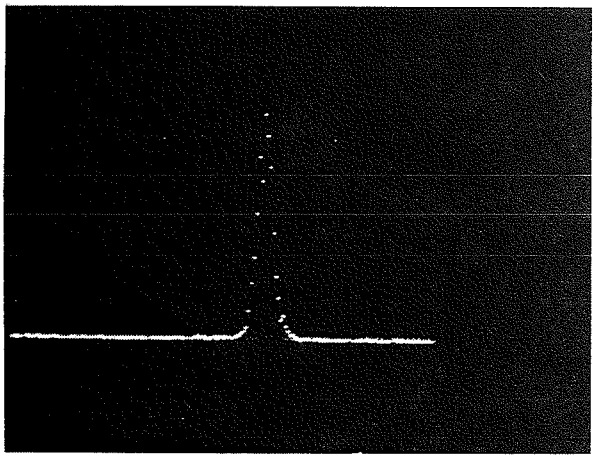

c)

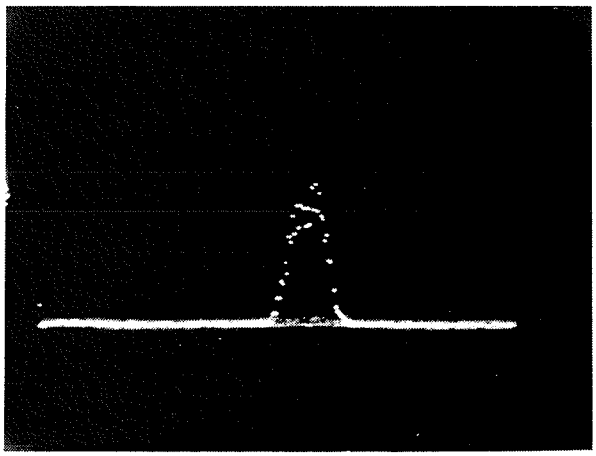

d)

Fig. 8

a)


b)

Fig. 9

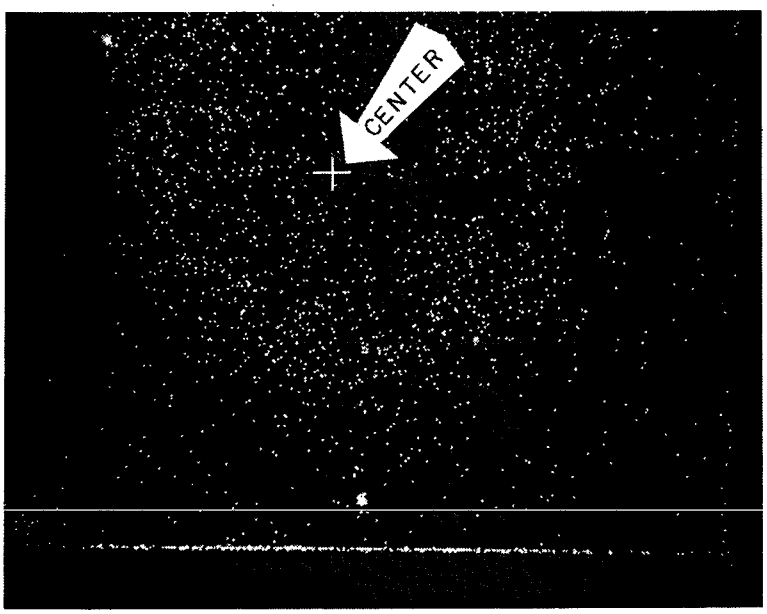


Fig. 10

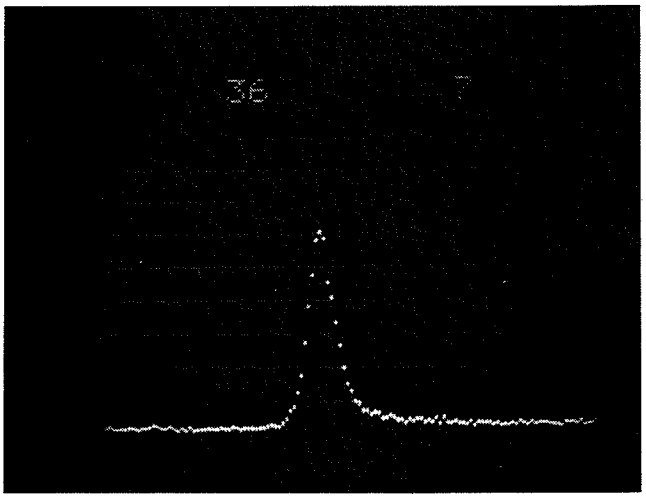

FWHM ≃ 800 μm

Fig. 11